Potential Energy Surfaces for Proton Abstractions from Acetic Acid

Mark S. Gordon,*,† David R. Gano,‡ and Eugene Curtiss‡

Contribution from the Department of Chemistry, Ames Laboratory−USDOE, Iowa State University, Ames, Iowa 50011, and Department of Chemistry, Minot State University, Minot, North Dakota 58707

Received November 17, 1995[⊗]

Abstract: The abstractions of hydrogen from both carbon and oxygen in acetic acid by hydride, fluoride, and hydroxide anions have been studied using *ab initio* electronic structure calculations. Molecular structures were optimized at the Hartree−Fock level of theory using the 6-31++G(d,p) basis set. For energetics, the 6-311++G(d,p) basis set was used, with second- and fourth-order perturbation theory corrections, for both minima and transition states. For the hydride and fluoride ion abstractions of hydrogen from carbon, a small activation energy exists at the Hartree−Fock level, but vanishes when correlation energy corrections are introduced. No other barriers are found for the abstraction reactions, but intermediate minima are found on the $F^- + CH_3COOH \rightarrow FH + {}^-CH_2COOH$ surface and on the analogous $OH^- + CH_3COOH$ surface. The calculated heats of formation for both acetic acid anions are in good agreement with the experimental values. The fourth-order perturbation theory calculation of the activation energy for the isomerization of acetate to enolate ion is 50.4 kcal/mol. The G2 values for the gas phase acidities of acetic acid at the OH and CH ends of the molecule are 339.3 and 365.8 kcal/mol, respectively. The former result is in good agreement with experiment.

I. Introduction

Acetic acid has two distinct types of hydrogen. One set of hydrogens is bonded to the methyl carbon, and one hydrogen is bonded to the carboxyl oxygen. When acetic acid loses a proton in an acid−base reaction, it had been thought[1] that it lost the proton bound to the oxygen atom, with the other three remaining bound to the carbon. However, in a recent study by O'Hair *et al.*[2] it was shown that the acetic acid enolate anion (**I**) can be readily prepared in a tandem flowing afterglow-selected ion flow tube by the reaction shown in eq 1. These

$$F^- + (CH_3)_3SiCH_2CO_2H \rightarrow CH_2COOH^- + (CH_3)_3SiF \quad (1)$$

authors have shown that the acetate ion, CH_3COO^- (**II**), and the enolate ion undergo quite different reactions, and from consideration of the collisional activation and charge reversal mass spectra of the ions they have shown that they are interconvertible *via* 1,3 proton transfer.

Grabowski and Cheng[3] discovered in their flowing afterglow experiments that when hydroxide reacts with CD_3COOH, 60% of the abstraction occurs from the carbon and 40% from the oxygen. Fluoride ion will also abstract 24% from the carbon and 76% from the oxygen. These studies indicate that there is indeed competition for abstraction from the hydrogens bound to carbon and the hydrogen bound to oxygen.

In this paper we present the results of *ab initio* electronic structure studies for the six reactions listed below.

$$F^- + CH_3COOH \rightarrow HF + CH_3COO^- \quad (2)$$

$$F^- + CH_3COOH \rightarrow HF + CH_2COOH^- \quad (3)$$

$$H^- + CH_3COOH \rightarrow H_2 + CH_3COO^- \quad (4)$$

$$H^- + CH_3COOH \rightarrow H_2 + CH_2COOH^- \quad (5)$$

$$OH^- + CH_3COOH \rightarrow H_2O + CH_3COO^- \quad (6)$$

$$OH^- + CH_3COOH \rightarrow H_2O + CH_2COOH^- \quad (7)$$

The fluoride, hydride, and hydroxide ions act as bases by abstracting hydrogens from either the oxygen, forming acetate ions, or the carbon, forming enolate ions. The barriers for the isomerization of acetate to enolate ion and for the OH rotation in enolate are also calculated. In addition, the Gaussian-2 model[4] is used to predict the heats of formation of enolate and acetate anions. The gas phase acidities for acetic acid donating a proton to form either acetate or enolate ion are calculated.

II. Computational Approach

Optimized geometries for the stationary points were obtained at the restricted Hartree−Fock (RHF) level, using the 6-31++G(d,p)[5] basis set and the Schlegel optimization method[6] in Gaussian88[7] and Gaussian92.[8] Some optimizations were done using the Baker[9] algorithim, an option in the GAMESS[10]

† Iowa State University.
‡ Minot State University.

(1) Bell, R. P. *The Proton In Chemistry*; Cornell University Press: Ithaca, NY, 1973.
(2) O'Hair, R. A. J.; Gronert, S.; Depuy, C. H.; Bowie, J. H. *J. Am. Chem. Soc.* **1989**, *111*, 3105−3106.
(3) Grabowski, J. J.; Cheng, X. *J. Am. Chem. Soc.* **1989**, *111*, 3106−3108.
(4) Curtiss, Larry A.; Raghavachari, K.; Trucks, G. W.; Pople, J. A. *J. Chem. Phys.* **1991**, *94*(11), 7221.
(5) (a) Hehre, W. J.; Ditchfield, R.; Pople, J. A. *J. Chem. Phys.* **1972**, *56*, 2257−2261. (b) Francl, M. M.; Pietro, W. J.; Hehre, W. J.; Binkley, J. S.; Gordon, M. S.; Defrees, D. J.; Pople, J. A. *J. Chem. Phys.* **1982**, *77*, 3654−3665. (c) Clark, T.; Chandrasekhar, J.; Spitznagel, G. W.; Schleyer, P. von R. *J. Comput. Chem.* **1983**, *4*, 294−301. (d) Spitznagel, G. W. Diplomarbeit, Erlangen, 1982. (e) Frisch, M. J.; Pople, J. A.; Binkley, J. S. *J. Chem. Phys.* **1984**, *80*, 3265−3269.
(6) Schlegel, H. B. *J. Comput. Chem.* **1982**, *3*, 214.

S0002-7863(95)03854-6 CCC: $12.00

suite of electronic structure algorithms. Minima and transition states were verified by establishing that the matrices of energy second derivatives (hessians) have zero and one negative eigenvalue, respectively. Energy differences (ΔE) augmented by the difference in vibrational zero-point energy (ZPE) give rise to the 0 K reaction enthalpy ΔH. (Since vibrational frequencies obtained in this manner are systematically too high, the ZPEs are multiplied by a scale factor of 0.8929.[11])

The reaction energetics were determined using second- and fourth-order Moller−Plesset[12] perturbation theory corrections to the RHF wave functions with the 6-311++G(d,p)[13] basis set, including the effects of triple excitations at the fourth-order level. Gaussian-2[4] was employed to calculate the heats of formation of the enolate and acetate ions.

The intrinsic reaction coordinate (IRC) is the minimum energy path connecting reactants and products *via* the transition state. The IRC provides additional evidence that a particular set of reactants is connected *via* a particular transition state to a set of products. The IRC was calculated for the acetate to enolate isomerization reaction using the second-order Gonzalez−Schlegel[14,15] (GS2) method implemented into GAMESS, with a step size of 0.30 bohr·amu$^{1/2}$.

III. Results and Discussion

In Table 1 the 6-311++G(d,p) energies for the minima and transition states are tabulated. These were employed in the calculation of the relative energies, as well as the enthalpy changes for the reactions. Those results are presented in Table 3 and will be discussed below.

Table 2 lists the geometric parameters for the minima and transition states. The geometries of H_2, H_2O, and HF are described elsewhere[16] and are not included in Table 2. The equilibrium geometries of enolate,[17] acetate, and acetic acid[18] have been reported by O'Hair *et al*. and Masamura, respectively, but are included in Table 2 and Figure 1 for convenience. The geometries reported in the literature for these species are almost exactly the same as the values that were obtained in our study. It is interesting that both C−O bond lengths in the acetate structure are quite short, ∼1.24 Å (cf. 1.19 and 1.33 Å in acetic acid); however the calculated bond orders for these bonds are 1.5, giving the expected coordination of four for the carboxyl carbon.

Table 1. 6-311++G(d,p)//RHF/6-31++G(d,p) Energies (hartrees) for Minima and Transition States

ion/molecule	RHF	MP2	MP4	ZPE[a]
		Minima		
H^-	−0.486 963	−0.505 611	−0.512 849	
F^-	−99.445 656	−99.678 687	−99.684 425	
H_2	−1.132 503	−1.160 280	−1.167 718	6.6
HF	−100.053 276	−100.278 647	−100.285 969	6.4
OH^-	−75.405 729	−75.639 912	−75.649 710	5.8
H_2O	−76.053 393	−76.274 187	−76.286 426	14.5
CH_3COOH	−227.883 469	−228.566 079	−228.615 877	41.7
CH_3COO^-	−227.307 612	−228.000 585	−228.048 350	32.4
CH_2COOH^-	−227.266 626	−227.960 266	−228.006 081	32.3
F^- min1	−327.352 453	−328.271 591	−328.327 882	41.9
F^- min2	−327.350 361	−328.275 553	−328.328 780	40.8
H^- min	−228.380 905	−229.085 796	−229.142 933	42.5
CH_2COOH^- [b]	−227.260 842	−227.954 654	−228.000 627	31.9
OH^- min	−303.312 104	−304.293 138	−304.233 007	48.3
		Transition State Structures		
F^- TS	−327.344 185	−328.274 183	−328.328 674	38.5
H^- TS	−228.361 986	−229.089 831	−229.144 463	39.8
isom[c]	−227.203 291	−227.915 703	−227.962 642	28.6
rot[d]	−227.253 036	−227.948 388	−227.994 666	31.6

[a] Zero-point vibrational energy in kcal/mol. [b] OH bond rotated 180°. [c] Transition state for acetate to enolate isomerization. [d] Transition state for 180° rotation of OH bond of enolate anion.

A. Abstraction by F^-. The geometries along the $F^- + CH_3COOH \rightarrow HF + {}^-CH_2COOH$ reaction path are presented in Figure 2. At the RHF/6-31++G(d,p) level of theory, two minima (min1, min2) separated by a transition state (TS) are found. Min1 is an ion−dipole complex, with a $F^-{-}H_5$ distance of 1.725 Å. The charge in this species resides primarily on F. The $C_1{-}H_5$ distance (1.116 Å) is just a bit longer than the normal equilibrium distance (1.08 Å) for a C−H bond. At the transition state (Figure 2b) the F−H bond is partially formed ($R(F{-}H_5) = 1.17$ Å) and $C_1{-}H_5$ is partially broken (1.371 Å). The $C_1{-}C_2$ distance is contracted to 1.448 Å, a value intermediate between those for normal C−C single and double bonds. At min2 (Figure 2c), the $H_5{-}F_9$ distance is 0.956 Å, very near its equilibrium distance in H−F. The C−H bond (1.838 Å) is essentially broken at this point. The $C_1{-}C_2$ bond length is 1.405 Å and is approaching the equilibrium distance in enolate (1.374 Å). The geometry of the substrate is almost the same as that of the enolate ion in this structure.

While min1, TS, and min2 are all stationary points at the RHF level of theory, addition of electron correlation (MP2 or MP4) changes the reaction path, such that it is downhill from the reactants to min2 and then increases in energy to the products. This is illustrated in Tables 1 and 3, as well as in Scheme 1a. So, when either MP2 or MP4 is used, min2 is the only remaining intermediate stationary point and is in fact the global minimum on the $F^- + CH_3COOH$ potential energy surface. As shown in Table 3, the overall reaction to produce FH + enolate is endothermic by 4.5 kcal/mol (MP4), while the intermediate complex is *exothermic* by ∼20 kcal/mol.

The reaction at the carboxyl end of acetic acid is much simpler, with a monotonic decrease in energy for the entire reaction path. This was established by a series of RHF/6-31++G(d,p) geometry optimizations, followed by MP2 and MP4 single points. So, there is no barrier for the abstraction

(7) Frisch, M. J.; Head-Gordon, M.; Schlegel, H. B.; Raghavachari, K.; Binkley, J. S.; Gonzalez, C.; Defrees, D. J.; Fox, D. J.; Whiteside, R. A.; Seeger, R.; Melius, C. F.; Baker, J.; Kahn, L. R.; Stewart, J. J. P.; Fluder, E. M.; Topiol, S.; Pople, J. A. *Gaussian 88*; Gaussian, Inc.: Pittsburgh, PA, 1988.

(8) Frisch, M. J.; Trucks, G. W.; Head-Gordon, M.; Gill, P. M. W.; Wong, M. W.; Foresman, J. B.; Johnson, B. G.; Schlegel, H. B.; Robb, M. A.; Replogle, E. S.; Gomperts, R.; Andres, J. L.; Raghavachari, K.; Binkley, J. S.; Gonzalez, C.; Martin, R. L.; Fox, D. J.; Defrees, D. J.; Baker, J.; Stewart, J. J. P.; Pople, J. A. *Gaussian 92, Revision A*; Gaussian, Inc.: Pittsburgh, PA, 1992.

(9) Baker, J. *J. Comput. Chem*. **1986**, *7*, 385−395.

(10) (a) Dupuis, M.; Spangler, D.; Wendoloski, J. J. *National Resource for Computations in Chemistry Software Catalog*; University of California: Berkeley, CA, 1980; Program QG01. (b) Schmidt, M. W.; Baldridge, K. K.; Boatz, J. A.; Jensen, J. H.; Koseki, S.; Gordon, M. S.; Nguyen, K. A.; Windus, T. L.; Elbert, S. T. *Quantum Chemistry Program Exchange Bulletin*, **1990**, *10*, 53−54. (c) Schmidt, M. W.; Baldridge, K. K.; Boatz, J. A.; Elbert, S. T.; Gordon, M. S.; Jensen, J. H.; Koseki, K.; Matsunaga, N.; Nguyen, K. A.; Su, S.; Windus, T. L.; Dupuis, M.; Montgomery, J. A., Jr. *J. Comput. Chem*. **1993**, *14*, 1347.

(11) Pople, J. A.; Schlegel, H. B.; Raghavachari, K.; De Frees, D. J.; Binkley, J. S.; Frisch, M. J.; Whiteside, R. A.; Hout, R. J. *Int. J. Quantum Chem. Symp*. **1981**, *515*, 269.

(12) (a) Pople, J. A.; Seeger, R.; Krishnan, R. *Int. J. Quantum Chem*. **1979**, *S11*, 149. (b) Krishnan, R.; Frisch, M. J.; Pople, J. A. *J. Chem. Phys*. **1980**, *72*, 4244.

(13) Krishnan, R.; Binkley, J. S.; Seeger, R.; Pople, J. A. *J. Chem. Phys*. **1980**, *72*, 650−654.

(14) Gonzales, C.; Schlegel, H. B. *J. Phys. Chem*. **1990**, *94*, 5523−5527.

(15) Gonzales, C.; Schlegel, H. B. *J. Chem. Phys*. **1991**, *95*, 5853−5860.

(16) Hehre, W. J.; Radom, L.; Schleyer, P. v. R.; Pople, J. A. *Ab Initio Molecular Orbital Theory*; John Wiley and Sons, Inc.: New York, NY, 1986.

(17) O'Hair, R. A. J.; Gronert, S.; DePuy, C. H.; Bowie, J. H. *J. Am. Chem. Soc*. **1989**, *111*, 3105−3106.

(18) Masamura, M. *Theor. Chim. Acta* **1989**, *75*, 433−446.

Table 2. RHF/6-31++G(d,p) Geometric Parameters for Minima and Transition States[a]

bond length[b]		bond angle		dihedral angle	
Equilibrium Geometry for CH_3COO^- (acetate ion)					
C_1C_2	1.546				
C_2O_3	1.239	$O_3C_2C_1$	114.9		
C_1H_4	1.088	$H_4C_1C_2$	109.5	$H_4C_1C_2O_3$	58.5
C_1H_5	1.088	$H_5C_1C_2$	109.5	$H_5C_1C_2O_3$	−58.5
C_1H_6	1.086	$H_6C_1C_2$	111.7	$H_6C_1C_2O_3$	180.0
C_2O_7	1.237	$O_7C_2C_1$	116.3	$O_7C_2C_1H_6$	0.0
Equilibrium Geometry for CH_2COOH^- (enolate ion)					
C_1C_2	1.374				
C_2O_3	1.244	$O_3C_2C_1$	130.7		
C_1H_4	1.074	$H_4C_1C_2$	119.3	$H_4C_1C_2O_3$	0.0
C_1H_5	1.075	$H_5C_1C_2$	120.8	$H_5C_1C_2O_3$	180.0
C_2O_6	1.391	$O_6C_2C_1$	115.0	$O_6C_2C_1O_3$	180.0
C_6H_7	0.944	$H_7O_6C_2$	103.7	$H_7O_6C_2O_3$	0.0
Geometry for CH_2COOH^- (OH Bond Rotated 180°)					
C_1C_2	1.389				
C_2O_3	1.227	$O_3C_2C_1$	129.8		
C_1H_4	1.078	$H_4C_1C_2$	122.0	$H_4C_1C_2O_3$	−180.0
C_1H_5	1.074	$H_5C_1C_2$	119.4	$H_5C_1C_2O_3$	0.0
C_2O_6	1.396	$O_6C_2C_1$	115.7	$O_6C_2C_1O_3$	180.0
O_6H_7	0.942	$H_7O_6C_2$	108.4	$H_7O_6C_2O_3$	−180.0
Equilibrium Geometry for CH_3COOH					
C_1C_2	1.501				
C_2O_3	1.189	$C_1C_2O_3$	125.7		
C_1H_4	1.079	$H_4C_1C_2$	109.5	$H_4C_1C_2O_3$	0.0
C_1H_5	1.084	$H_5C_1C_2$	109.5	$H_5C_1C_2O_3$	121.0
C_1H_6	1.084	$H_6C_1C_2$	109.5	$H_6C_1C_2O_3$	−121.0
C_2O_7	1.331	$O_7C_2C_1$	112.1	$O_7C_2C_1O_3$	180.0
H_8O_7	0.948	$H_8O_7C_2$	108.9	$H_8O_7C_2O_3$	0.0
Min1: $F^- + CH_3COOH$					
C_1C_2	1.486				
C_2O_3	1.199	$O_3C_2C_1$	127.1		
C_1H_4	1.083	$H_4C_1C_2$	108.9	$H_4C_1C_2O_3$	−19.1
C_1H_5	1.116	$H_5C_1C_2$	109.9	$H_5C_1C_2O_3$	101.0
C_1H_6	1.085	$H_6C_1C_2$	109.8	$H_6C_1C_2O_3$	−140.5
C_2O_7	1.341	$O_7C_2C_1$	113.4	$O_7C_2C_1O_3$	180.3
H_8O_7	0.946	$H_8O_7C_2$	107.3	$H_8O_7C_2O_3$	−4.9
F_9H_5	1.725	$F_9H_5C_1$	176.7	$F_9H_5C_1O_3$	−168.4
Min2: $F^- + CH_3COOH$					
C_1C_2	1.405				
C_2O_3	1.227	$O_3C_2C_1$	129.7		
C_1H_4	1.079	$H_4C_1C_2$	115.2	$H_4C_1C_2O_3$	−20.1
C_1H_5	1.838	$H_5C_1C_2$	107.3	$H_5C_1C_2O_3$	89.7
C_1H_6	1.079	$H_6C_1C_2$	116.6	$H_6C_1C_2O_3$	−161.9
C_2O_7	1.374	$O_7C_2C_1$	114.5	$O_7C_2C_1O_3$	182.8
H_8O_7	0.945	$H_8O_7C_2$	104.9	$H_8O_7C_2O_3$	−2.6
F_9H_5	0.956	$F_9H_5C_1$	174.1	$F_9H_5C_1O_3$	−161.7
Min: $H^- + CH_3COOH$					
C_1C_2	1.493				
C_2O_3	1.196	$O_3C_2C_1$	126.5		
H_4C_1	1.081	$H_4C_1C_2$	109.3	$H_4C_1C_2O_3$	−13.9
H_5C_1	1.092	$H_5C_1C_2$	110.1	$H_5C_1C_2O_3$	106.1
H_6C_1	1.084	$H_6C_1C_2$	110.0	$H_6C_1C_2O_3$	−135.8
C_2O_7	1.336	$O_7C_2C_1$	112.9	$O_7C_2C_1O_3$	−179.9
H_8O_7	0.947	$H_8O_7C_2$	107.9	$H_8O_7C_2O_3$	−4.4
H_9H_5	2.316	$H_9H_5C_1$	169.6	$H_9H_5C_1O_3$	−159.6
Saddle Point: $F^- + CH_3COOH$					
C_1C_2	1.448				
C_2O_3	1.211	$O_3C_2C_1$	128.5		
H_4C_1	1.084	$H_4C_1C_2$	110.6	$H_4C_1C_2O_3$	−25.8
H_5C_1	1.371	$H_5C_1C_2$	109.9	$H_5C_1C_2O_3$	92.1
H_6C_1	1.084	$H_6C_1C_2$	111.8	$H_6C_1C_2O_3$	−151.6
C_2O_7	1.358	$O_7C_2C_1$	114.0	$O_7C_2C_1O_3$	−177.3
H_8O_7	0.946	$H_8O_7C_2$	106.0	$H_8O_7C_2O_3$	−3.6
F_9H_5	1.170	$F_9H_5C_1$	176.1	$F_9H_5C_1C_2$	170.8
Saddle Point: $H^- + CH_3COOH$					
C_1C_2	1.438				
C_2O_3	1.213	$O_3C_2C_1$	128.4		
H_4C_1	1.081	$H_4C_1C_2$	112.7	$H_4C_1C_2O_3$	−24.8
H_5C_1	1.378	$H_5C_1C_2$	107.8	$H_5C_1C_2O_3$	89.6
H_6C_1	1.082	$H_6C_1C_2$	114.1	$H_6C_1C_2O_3$	−156.9
C_2O_7	1.359	$O_7C_2C_1$	113.9	$O_7C_2C_1O_3$	−175.1
H_8O_7	0.945	$H_8O_7C_2$	106.0	$H_8O_7C_2O_3$	−3.7
H_9H_5	1.117	$H_9H_5C_1$	175.7	$H_9H_5C_1O_3$	−157.8
Acetate/Enolate Isomerization Reaction Transition State Geometry					
C_1C_2	1.523				
C_2O_3	1.211	$O_3C_2C_1$	132.4		
H_4C_1	1.091	$H_4C_1C_2$	111.5	$H_4C_1C_2O_3$	60.7
H_5C_1	1.091	$H_5C_1C_2$	111.5	$H_5C_1C_2O_3$	−60.6
H_6C_1	1.471	$H_6C_1C_2$	65.7	$H_6C_1C_2O_3$	180.0
C_2O_7	1.310	$O_7C_2C_1$	101.7	$O_7C_2C_1H_6$	−0.0
Enolate Rotational Transition State Geometry					
C_1C_2	1.378				
C_2O_3	1.230	$O_3C_2C_1$	130.5		
H_4C_1	1.075	$H_4C_1C_2$	120.9	$H_4C_1C_2O_3$	175.5
H_5C_1	1.076	$H_5C_1C_2$	119.4	$H_5C_1C_2O_3$	1.5
C_2O_6	1.423	$O_6C_2C_1$	113.9	$O_6C_2C_1O_3$	179.6
H_7O_6	0.942	$H_7O_6C_2$	107.4	$H_7O_6C_2O_3$	97.6
$OH^- +$ Acetic Acid (Min)					
C_1C_2	1.500				
C_2O_3	1.195	$O_3C_2C_1$	121.9		
H_4C_1	1.072	$H_4C_1C_2$	110.3	$H_4C_1C_2O_3$	25.8
H_5C_1	2.122	$H_5C_1C_2$	113.0	$H_5C_1C_2O_3$	174.5
H_6C_1	1.087	$H_6C_1C_2$	109.4	$H_6C_1C_2O_3$	−96.6
O_7C_2	1.318	$O_7C_2C_1$	113.8	$O_7C_2C_1O_3$	−187.7
H_8O_7	0.950	$H_8O_7C_2$	109.6	$H_8O_7C_2O_3$	−3.3
O_9H_5	0.999	$O_9H_5C_1$	37.3	$O_9H_5C_1O_3$	−96.1
$H_{10}O_9$	0.992	$H_{10}O_9H_5$	114.1	$H_{10}O_9H_5O_3$	114.0

[a] The atom numbering system is given in Figure 1. [b] Bond lengths in angstroms, angles in degrees.

of hydrogen from the hydroxyl group by fluoride ion. Both MP4 and G2 predict that this reaction is exothermic by 22 kcal/mol (Table 3). This is within 1 kcal/mol of the experimental value. Note that at the MP4/6-311++G(d,p) level of theory min2 is essentially isoenergetic with $HF + CH_3COO^-$, even though enolate is much higher in energy than acetate.

B. Abstraction by H^-. Because H^- is much less stable than F^-, the reaction of H^- with CH_3COOH to produce $^-CH2COOH + H_2$ is rather exothermic, by nearly 30 kcal/mol as shown in Table 3. At the RHF level of theory, an intermediate complex and transition state are found on this reaction path. These two intermediate structures are shown in Figure 3, but it is clear from Table 3 and Scheme 1b that these stationary points disappear at correlated levels of theory. So, this reaction is predicted to proceed steadily downhill to products, with no intervening barrier.

Table 3. Relative Energies (kcal/mol)

	min1		TS		min2							
reaction[a]	ΔE	ΔH_0	ΔE	ΔH_0	ΔE	ΔH_0	ΔE	ΔH_{298}	ΔH_{exp}[b]	G2[c]	$\Delta 1$[d]	$\Delta 2$[e]
H^- to enolate	−6.6	−5.9	5.3	3.6			−18.0	−18.5	−32.6 ± 3.2	−28.4	14.1	4.2
	−8.8	−8.1	−11.4	−13.1			−30.7	−31.2			1.4	
	−8.9	−8.2	−9.9	−11.6			−28.3	−28.8			3.8	
H^- to acetate							−43.7	−44.0	−52.1 ± 3.0	−52.9	8.1	−0.8
							−56.0	−56.3			−4.2	
							−54.8	−55.1			−3.0	
F^- to enolate	−14.6	−14.5	−9.4	−12.3	−13.3	−14.1	5.8	5.1	−2.8 ± 3.2	1.4	7.9	4.2
	−16.8	−16.7	−18.5	−21.4	−19.3	−20.1	3.7	3.0			5.8	
	−17.3	−17.2	−17.8	−20.7	−17.9	−18.7	5.2	4.5			7.3	
F^- to acetate							−19.9	−20.4	−22.3 ± 3.0	−23.1	1.9	−0.8
							−21.6	−22.1			0.2	
							−21.4	−21.9			0.4	
OH^- to enolate					−14.4	−13.7	−19.3	−19.8	−22.6 ± 3.2	−18.4	2.8	4.2
					−17.0	−16.3	−17.9	−18.3			4.3	
					−17.3	−16.6	−16.9	−17.3			5.3	
OH^- to acetate							−45.1	−45.3	−42.1 ± 3.0	−42.9	−3.2	−0.8
							−43.2	−43.4			−1.3	
							−43.4	−43.6			−1.5	
acetate to enolate			65.5	62.1			25.7	25.4	19.4 ± 4.4	24.5	5.9	5.0
			53.3	49.9			25.3	25.0			6.5	
			53.8	50.4			26.5	26.2			6.7	
enolate (OH rotation)			8.5	7.9			3.6	3.2				
			7.5	6.9			3.5	3.1				
			7.2	6.6			3.4	3.0				

[a] For each reaction the numbers in the first line were calculated using RHF/6-311++G(d,p), the second using MP2/6-311++G(d,p), and the third using MP4/6-311++G(d,p). [b] See Table 4 for the experimental values of ΔH_f used in the calculation of ΔH_{exp}. [c] The numbers in this column were calculated using the Table 4 values of ΔH_f for all species except the acetate and enolate ions, whose ΔH_f values were calculated using G2 theory. [d] $\Delta 1 = \Delta H_{298} - \Delta H_{exp}$ [e] $\Delta 2 = G2 - \Delta H_{exp}$

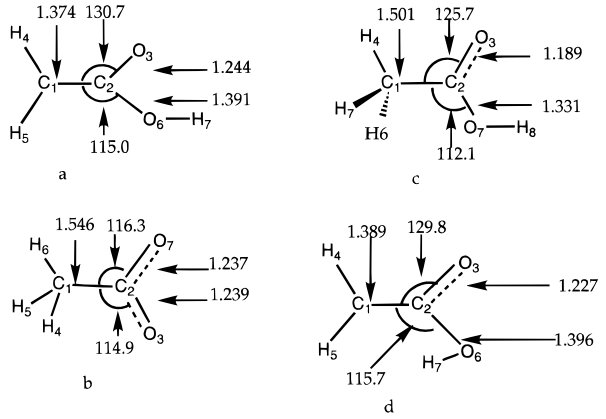

Figure 1. Schematics of RHF/6-31++G(d,p) geometries (bond lengths in Å, angles in degrees). (a) Enolate ion. (b) Acetate ion. (c) Acetic acid. (d) Enolate ion with OH bond rotated 18°.

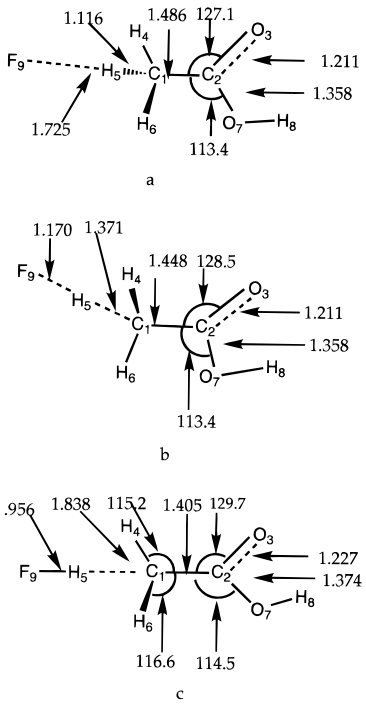

Figure 2. Geometries along the $F^- + CH_3COOH \rightarrow HF + {}^-CH_2COOH$ reaction path (bond lengths in Å, angles in degrees). (a) Min1. (b) TS. (c) Min2.

As in the fluoride ion reaction, no barrier was found for the abstraction of the hydroxyl group hydrogen. The calculated reaction enthalpy (Table 3: −55 kcal/mol) is almost double that found for the reaction that produces enolate anion. The heat of formation of acetate ion is about 25 kcal/mol more exothermic than that of enolate ion, and this is clearly the difference.

C. Abstraction by OH^-. Linear synchronous transit calculations using the procedure described above for F^- show that the reaction of hydroxide ion with acetic acid at either end of the molecule is energetically downhill all the way to products. No barrier is found for either reaction. A search for a minimum along the path to enolate anion produced the structure shown in Figure 4c. The geometry of this structure appears to be a complex between a water molecule and the enolate fragment. Indeed, the structure of this species (Table 2) suggests a well-formed water molecule with short OH distances (H_5-O_9, $H_{10}-O_9$) and an HOH angle of 114°. However, the C_1-O_9 distance (1.46 Å) is shorter than one would expect for a weakly bound complex, and the OH^- has transferred only about 25% of the negative charge to the enolate in this structure. Thus, it is not so surprising that the enthalpy change of this "minimum" on the potential energy surface relative to reactants at the MP4 level of theory is almost the same as the net ΔH for the reaction that produces enolate.

The production of H_2O + enolate is predicted to be much less exothermic (18 vs 43 kcal/mol) than the production of

Scheme 1. Schematic Potential Energy Profiles[a]

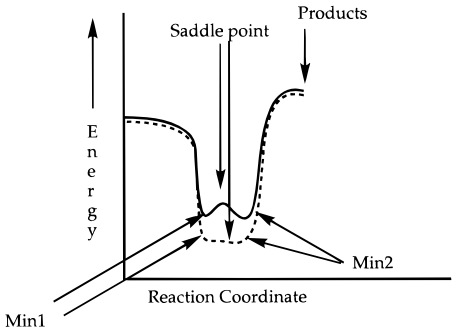

a

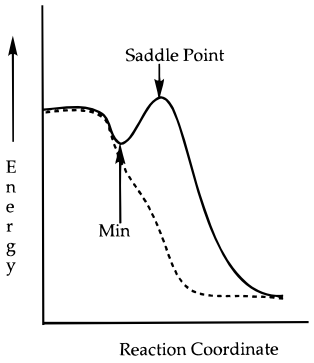

b

[a] Solid line = RHF level of theory. Dashed line = MP4 level of theory. (a) F^- + acetic acid. (b) H^- + acetic acid.

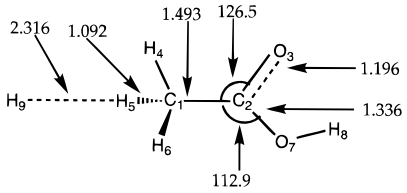

a

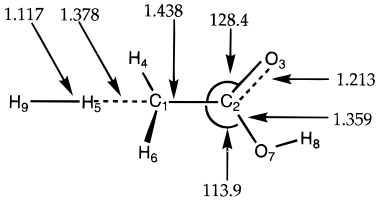

b

Figure 3. Structures on the H^- + CH_3COOH reaction path (bond lengths in Å, angles in degrees). (a) H^- + CH_3COOH (min). (b) H^- + CH_3COOH (TS).

acetate. Again, this is due to the more negative heat of formation for the acetate ion.

D. Isomerization of Acetate to Enolate. The symmetry of the transition state for the isomerization of acetate to enolate (Figure 4a) is C_S. The C_1-C_2 distance (1.523 Å) is slightly shorter than its distance in the acetate anion, while the $O_3C_2C_1$ angle has opened to 132.4° and is about 2° larger than its value in the enolate anion. The H_6-C_1 distance is lengthened to 1.471 Å and is much longer than that of a normal C−H bond. The angle, $H_6C_1C_2$, has closed from 111.7° in the acetate anion to a value of 65.7° at the TS. The O_7-C_2 distance has increased and is approaching that of a normal C−O single bond. The $O_7C_2C_1$ angle has closed to 101.7°. This combination of moves places H_6 within 1.184 Å of O_7, which is approaching the equilibrium OH bond distance of about 0.95 Å. In proceeding

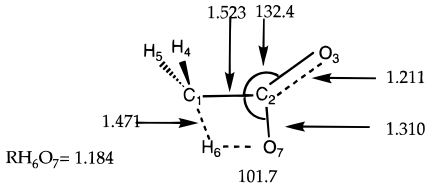

a

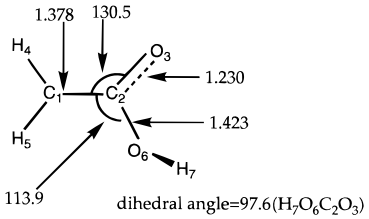

b

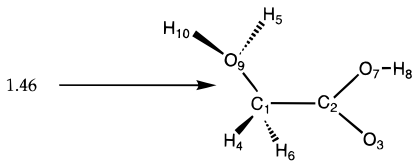

c

Figure 4. Transition state structures (bond lengths in Å, angles in degrees). (a) Acetate/enolate isomerization TS. (b) Enolate OH rotation TS. (c) OH^- + acetic acid (min).

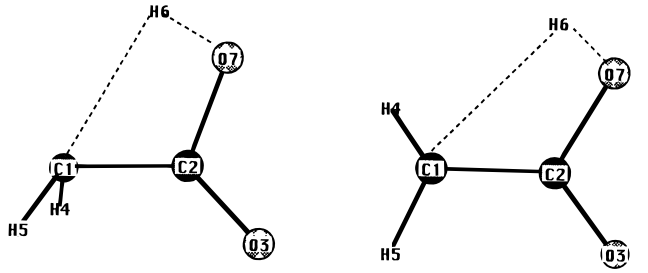

a b

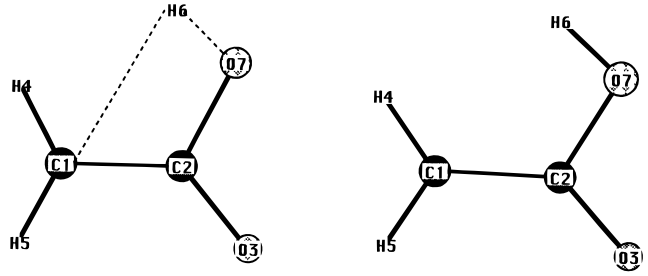

c d

Figure 5. Points along the forward IRC for the acetate to inolate isomerization reaction. (a) TS. (b) Point 15 forward. (c) Point 19 forward. (d) Final point forward (min).

from the TS along the forward IRC (Figure 5a−d), viewing from C1 to C2 along the C1−C2 bond, H_4 and H_5 gradually rotate clockwise into the plane of the molecule.

The activation energy for the acetate to enolate isomerization, (Table 3 and Scheme 2) is predicted to be about 50 kcal/mol, at both the MP2 and MP4 levels of theory, using the 6-311++G(d,p) basis set. Thus, the isomerization of acetate to enolate will be a slow process and is not likely to play an important role in the abstraction reactions. Since the isomerization of acetate to enolate is endothermic by 25−26 kcal/mol, the activation energy for the reverse reaction is around 25 kcal/mol.

Scheme 2. Schematic Potential Energy Profile for the Acetate to Enolate Isomerization Reactions[a]

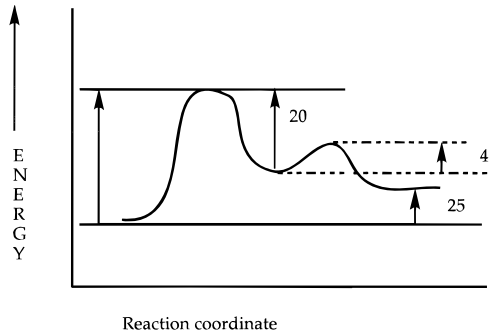

[a] The numbers are rounded from Table 3.

Table 4. Heats of Formation[a] Used for Calculating ΔH_{exp} (All kcal/mol)

species	$\Delta H°_f$
H^+	367.2
F^-	-59.6 ± 0.3
H^-	-59.6 ± 0.0
OH^-	-32.8 ± 0.2
H_2O	-57.8 ± 0.01
HF	-64.8 ± 0.2
CH_3COOH	-103.3 ± 0.1 (-102.3)
CH_3COO^-	-120.4 ± 3.0 (-121.2)
CH_2COOH^-	-100.9 ± 3.2 (-96.7)

[a] All values from ref 19 except H^+, which is from ref 20. [b] Values in parentheses were calculated with G2.

E. Enolate (Rotation of the OH Bond). When the intrinsic reaction coordinate (IRC)[14,15] is pursued in the forward direction from the isomerization transition state, the product is enolate with the OH bond rotated by 180°. The rotational transition state was found to have a geometry (Figure 4b) that is quite similar to the geometries of both enolate and its higher energy conformation. In this TS the dihedral angle $H_7O_6C_2O_3$ is 97.6° compared with 0° in enolate and 180° in the rotational conformer. The C_2-O_6 bond length (1.423 Å) is slightly longer than that in enolate or in the higher energy structure. The MP4 barrier height (Table 3) for the OH bond rotation is 7.2 kcal/mol, while the enthalpy change (activation energy) for this reaction is 6.6 kcal/mol. A schematic potential energy profile for the isomerization reaction including the rotation of the OH bond is shown in Scheme 2.

F. Comparison with Experiment. 1. Enthalpies of Reaction. In Table 3, the column under ΔH_{exp} contains the values of the enthalpies of reaction determined from experimental standard enthalpies of formation (Table 4). The values in the column labeled ΔH_{298} were calculated using the appropriate calculated energy values from Table 1. The column labeled $\Delta 1$ is the error ($\Delta H_{298} - \Delta H_{exp}$) for the results of each reaction. The average error at the MP4 level of theory is 4.0 kcal/mol. The average uncertainty in the experimental enthalpies of reaction is ±3.3 kcal/mol, so there is very good agreement between the calculated and experimental enthalpies of reaction.

The G2 standard heats of formation for acetate ion, enolate ion, and acetic acid were found to be −121.2, −96.7, and −102.3 kcal/mol, respectively, in comparison with the experimental values of -120.4 ± 3.1, -100.9 ± 3.2, and -103.3 ± 0.1 kcal/mol. This is in excellent agreement with the experimental values for acetate and acetic acid, and it is almost within the experimental error range for enolate. Previous G2(MP2)[21] values of −124.8 and −105.8 kcal/mol were reported[22] for the heats of formation of acetate ion and acetic acid, respectively.

When the foregoing G2 results are substituted for acetate and enolate in the calculation of the experimental reaction enthalpies, the column labeled G2 of Table 3 is the result and $\Delta 2$ is the error between G2 and ΔH_{exp}. The average error is 2.9 kcal/mol, giving very good agreement with the experimental enthalpies of reaction.

2. Activation Energies. To our knowledge, there are no experimentally determined activation energies for any of the reactions studied here. However, Grabowski and Cheng[3] found that both fluoride and hydroxide abstracted hydrogens from both the carboxyl oxygen and the methyl group of acetic acid. This suggests that if activation energies exist, they are not large. Our results are consistent with this. Bowie[23] *et al*. calculated a barrier of 56 kcal/mol for a 1,2 H transfer in CH_3CO^- to form the acetaldehyde enolate ion, and they expected that the 1,3 H transfer in acetate ion would be lower. Again, this is consistent with our value of 50 kcal/mol.

3. Gas Phase Acidities. The gas phase acidities for the ionization of acetic acid producing enolate and acetate at the MP4, MP2, and G2 levels are compared with experiment in Table 5. The values for the reaction producing acetate are in good agreement with experiment.

Table 5. Gas Phase Acidities for OH and CH of Acetic Acid (kcal/mol)

method	OH	CH
MP4/6-311++G(d,p)	338.3	366.4
MP2/6-311++G(d,p)	337.1	363.9
G2	340.0	365.8
experimental[a]	341 ± 3.0	363 ± 3.2
experimental[b]	341.5	361.2

[a] Calculated from standard enthalpies of formation and the equation, $\Delta G = \Delta H - T\Delta S$. ΔS was obtained from statistical mechanics calculations. [b] Reference 3.

IV. Summary

At the highest levels of theory, it is found that there are no activation energies for proton abstraction from acetic acid at either C or O by F^-, OH^-, or H^-. On the F^- surface leading to enolate, there is a minimum that is essentially isoenergetic with FH + acetate. So, while acetate is much more stable than enolate, the intermediate minimum on the enolate pathway makes the two alternatives quite competitive. There is an analogous minimum on the OH^- + acetate potential energy surface. While this minimum is essentially isoenergetic with enolate + water, it is still much higher in energy than the alternative products acetate + water. Stable ion−molecule complexes such as those found in this study appear to be commonplace in ion−molecule reactions. Similar complexes have been found on the potential energy surfaces for reactions of both anions[24] and cations,[25] and they also may be expected for reactions involving highly polar neutral species.[26] The

(19) Bartmess, J. E. NIST Negative Ion Energetic Database, Version 3.0, Nist Standard Reference Database 19B, NIST, 1993.
(20) Chase, M. W., Jr.; Davies, C. A.; Downey, J. R., Jr.; Frurip, D. J.; McDonald, R. A.; Syverud, A. N. *J. Phys. Chem. Ref. Data* **1985**, *14*, Suppl. no. 1.
(21) Curtiss, L. A.; Raghavachari, K.; Pople, J. A. *J. Chem. Phys*. **1993**, *98*, 1293.
(22) Yu, Dake; Rauk, A.; Aromstrong, D. A. *J. Chem. Chem. Soc., Perkin Trans*. **1994**, *2*, 2207.
(23) Downard, K. M.; Sheldon, J. C.; Bowie, J. H. *Int. J. Mass Spectrom. Ion Processes* **1988**, *86*, 217.
(24) (a) Schmidt, M. W.; Gordon, M. S. *J. Am. Chem. Soc*. **1991**, *113*, 5244. (b) Shimizu, H.; Gordon, M. S.; Damrauer, R.; O'Hair, R. A. J. *Organometallics* **1995**, *14*, 2664.
(25) Nguyen, K. A.; Gordon, M. S.; Raghavachari, K. *J. Phys. Chem*. **1994**, *98*, 6704.
(26) Gordon, M. S.; Barton, T. R. Manuscript in preparation.

existence of such complexes on the potential energy surfaces clearly plays an important role in the associated reaction dynamics. An investigation of the dynamics will be necessary to understand the observed branching ratio.[3]

The predicted heats of formation and reaction enthalpies are in very good agreement with experiment.

Acknowledgment. This work was supported by a Faculty Research Appointment to D.R.G. from Minot State University, by a grant to M.S.G. from the National Science Foundation (CHE9411911), by a summer research grant to D.R.G. from Ames Laboratory, and by Iowa State University. The calculations were performed on IBM RS/6000 workstations at North Dakota State University, Minot State University, and Iowa State University. The authors thank Dr. Michael Schmidt and Professor Joe Grabowski for many helpful discussions.

JA9538546